Revealing the Implied Risk-neutral MGF with the Wavelet Method

Emmanuel Haven*

Xiaoquan Liu†

Chenghu Ma‡

Liya Shen§

February 28, 2007

*Department of Accounting, Finance and Management, University of Essex, Colchester CO4 3SQ, UK. Phone: +44 1206 873768. Email: ehaven@essex.ac.uk.

†Department of Accounting, Finance and Management, University of Essex, Colchester CO4 3SQ, UK. Phone: +44 1206 873849. Email: liux@essex.ac.uk.

‡The Wang Yanan Institute for Studies in Economics, Xiamen University, Xiamen, P. R. China. Email: chmauk@yahoo.ca. Phone: +86 5922181602. Ma acknowledges funding from ESRC UK.

§Department of Accounting, Finance and Management, University of Essex, Colchester CO4 3SQ, UK. Email: lshenb@essex.ac.uk. Shen acknowledges funding from Overseas Research Students Awards Scheme (ORSAS), UK. This paper is part of her PhD thesis.

Abstract

Options are believed to contain unique information about the risk-neutral moment generating function (MGF hereafter) or the risk-neutral probability density function (PDF hereafter). This paper applies the wavelet method to approximate the risk-neutral MGF of the underlying asset from option prices. Monte Carlo simulation experiments are performed to elaborate how the risk-neutral MGF can be obtained using the wavelet method. The Black-Scholes model is chosen as the benchmark model. We offer a novel method for obtaining the implied risk-neutral MGF for pricing out-of-sample options and other complex or illiquid derivative claims on the underlying asset using information obtained from simulated data.

Keywords: Implied risk-neutral MGF; wavelets; options; Black-Scholes model.

JEL: G12; G13.

1 Introduction

In the early 1970s, Black and Scholes (1973) presented the classic Black-Scholes option pricing formula, which is one of the most important advances in option pricing. However, since the 1987 stock market crash, there is growing empirical evidence showing that the market differs from the Black-Scholes paradigm. There are mainly two types of stylized facts observed: (i) The Black-Scholes model assumes that the volatility of the underlying security is constant. However, empirical evidence shows the implied volatilities of real market options vary across strike prices and exhibit a smile or skew shape across the moneyness (strike/underlying asset price ratio); (ii) The Black-Scholes model assumes that the stock prices follow a geometric Brownian motion, thus the risk-neutral probability density function of the underlying asset is lognormal. However, researchers have observed excess kurtosis and negative skewness of unconditional returns of the underlying security which is inconsistent with the lognormality assumption. The first abnormality is indeed related to the second one, since statistics such as volatility, skewness, and kurtosis can be derived if we know the entire risk-neutral PDFs. Therefore, the central empirical issue in option pricing is what distributional hypothesis is consistent with underlying security prices and real market option prices. In our paper, we are interested in estimating the implied risk-neutral MGF. It needs to be stressed that to date, a lot of methods have been developed which have as purpose to extract the risk-neutral PDF. However, very little attention has been paid to the risk-neutral MGF.

In this paper we try to back out the risk-neutral MGF by using the wavelet method based on the option pricing formula derived by Ma (2006b).

Further details about the MGF, the wavelet method and the option pricing formula of Ma (2006b) will be provided in the following sections. The contributions of this paper are listed below.

1. Although there is one-to-one relationship between the MGF and the PDF, the MGF is more tractable in some cases. For instance, when there are random jumps in the process, the PDF will not have an explicit form, while for the MGF, we may expect an analytical expression (Ma and Vetzal, 1995).

2. The implied risk-neutral MGF obtained from our model is continuous while the implied risk-neutral PDF obtained from other methods such as the smoothed smile method is discrete.

3. With the risk-neutral MGF estimated, out-of-sample options with different time-to-maturity, different strike prices and even different underlying security prices can be calculated very easily. We note that existing estimation methods such as the volatility smile method and the double lognormal method aim to estimate the risk-neutral PDF, which can only be used to infer the distribution at one specific time. Therefore, the estimated PDF can only be used to price out-of-sample options with a same fixed expiry date. In this sense, estimating the risk-neurtal MGF is definitely more appealing from a practical point of view.

4. It is well known that option prices contain rich information on the implied volatility, the preference parameter, the jump process and the higher moments of the distribution. Based on the model developed by Ma (1992)and Ma (2006b), with the risk-neutral MGF estimated, in addition to the mean and variance, we are also able to obtain the skew-

ness and kurtosis of the underlying asset distribution directly from the risk-neutral MGF. Moreover, the preference parameter of the utility function can be revealed easily (Ma, 2006a, pg. 233-234).

5. There is no need to put any restrictions on the stochastic process of the underlying asset or put any prior assumptions on the implied risk-neutral MGF. This ensures the flexibility of this method in the first place. Furthermore, wavelets can be used to represent any square integrable functions. We note this is an advantage since the type of function is more restricted with other methods such as the polynomial or cubic spline method.

6. The wavelet method does not require a large collection of data for a reasonable level of accuracy as the kernel estimation method Ait-Sahalia and Lo (1998) does. We need only a small sample of options to estimate the implied risk-neutral MGF. For example, we can estimate the risk-neutral MGF using only nine options with different strike prices for a same underlying asset of some certain time-to-maturity and obtain a reasonably accurate risk-neutral MGF, while the kernel estimation method requires several thousand data points to obtain a reasonable level of accuracy.

7. Our technique avoids ill-posed inverse problems. According to Breeden and Litzenberger (1978), the risk-neutral PDF $g(X)$can be obtained by differentiating the option pricing formula twice with respect to the strike prices X. For example, let us suppose there are three European call option prices c_1, c_2, and c_3 with time to maturity τ and strike prices of $K-\delta$, K, and $K+\delta$ respectively. Suppose the annually risk free interest rate is r. The estimate of $g(X)$ at point $X = K$ is given

by $g(K) = e^{r\tau}\frac{c_1+c_3-2c_2}{\delta^2}$ provided that δ is a small number. However, there is a problem associated with this method, i.e, the second derivative of the estimator of the call pricing function may not be a good estimator for the second derivative of the true call pricing function. This is because the option prices used for estimation are subject to perturbations and the small errors of the option prices will be dramatically magnified when the denominator δ^2 is infinitely small. Using the model in Ma (2006b), we avoid this problem by transforming the problem into a least squares problem and we estimate the parameters of a linear series which make up of the risk-neutral PDF.

One may ask why the wavelet method is chosen instead of Fourier analysis. One of the reasons is that "in some cases (e.g. fingerprints) wavelet analysis is much better than Fourier analysis in the sense that fewer terms suffice to approximate certain functions" (Bachman, Narici, and Beckenstein, 2002, pg. 411). What's more, the Fourier series are a linear combination of a series of sine and cosine functions, which are defined over the entire real axis. Due to the properties of the components, i.e., sine and cosine functions are periodic, Fourier analysis is appealing in representing periodic functions. However, for non-periodic functions such as financial time series, the Fourier methodology is not favorable since there is no repetition within the sampled region. Wavelets, however, are not restricted to a fixed shape or fixed position. Therefore, wavelets are more effective in dealing with non-periodic function or non-stationary data series such as financial time series.

Wavelets, as a mathematical analysis tool, have been broadly applied in the engineering area such as data-compression, de-noising, edge-detection, earthquake prediction, and so on. However, it is to be noted that the use

of wavelets in finance and economics is only a recent phenomenon. Despite this, wavelets are a very useful tool in financial and economics analysis. We will provide some examples in the following context.

The rest of this paper is organized as follows. The next section deals with an overview of existing methods. We provide a brief overview on wavelets in section 3. Section 4 is divided into two parts. Some theoretical primitives on the risk-neutral MGF and on wavelets are presented respectively in this section. Section 5 describes the model and methodology of our paper. Simulation and experimental results are given in section 6. The last section comes with the summary and conclusions.

2 An overview of existing methods

The existing methods for revealing the risk-neutral PDF can be mainly grouped into two groups: parametric and nonparametric ones. While the parametric methods can again be mainly divided into three categories. We start first with parametric methods.

1. The first approach is to fit the call pricing function or the implied volatility smile curve parametrically. The risk-neutral PDF is then derived by implementing Breeden and Litzenberger (1978)'s result. To implement this approach, one needs equally spaced striking prices varying from zero to infinity continuously. However, option contracts are only traded at discrete strike prices and what's more, the strike prices are spanned over a very limited range either side of the at-the-money strike price. Therefore, most of the effort is focused on interpolating the option prices at equally spaced strike prices and extrapolating outside of the traded option prices range to estimate

the entire distribution. See for instance, Shimko (1993), Malz (1997), Bates (1991), and Bliss and Panigirtzoglou (2002).

2. The second approach is to specify a stochastic process for the underlying asset price and the parameters of the assumed process can be recovered by using the observed option prices, and therefore the risk-neutral PDF can be inferred from the stochastic process. For instance, the classic Black-Scholes 1973 model assumes that the stock prices follow the Geometric Brownian motion with a constant risk-free rate and constant volatility, and this implies a lognormal distribution for the stock prices. See more examples in Duffie, Pan, and Singleton (2000) and Bates (2000)for the jump-diffusion process and stochastic volatility model.

3. The third approach assumes a parametric form for the risk-neutral PDF of the underlying asset directly, and the parameters of the risk-neutral PDF can be estimated by minimizing the distance between the observed option prices and the fitted prices based on the model (least square method). For example, Melick and Thomas (1994) assume a mixture of three lognormal distributions for the terminal implied PDF, and the estimation is carried out using the bounds on the prices of American options. The mixture of the lognormal method is claimed as flexible, general and direct.

Another strand of the literature utilizes non-parametric methods. For non-parametric methods, one may achieve more flexibility since there are no prior restrictions on the stochastic process of the underlying asset prices, the call pricing function, or on the distribution function. For example, Rubinstein (1994) proposes a new method by establishing a prior parametric

distribution as a guess of the risk-neutral probabilities. The implied risk-neutral probability is then estimated by minimizing the distance between the implied distribution and the prior probability distribution, subject to the condition that the observed option prices are valued correctly based on the implied risk-neutral probabilities distribution. Rubinstein's approach is non-parametric in that any probability distribution is a possible solution. This method requires a large amount of options so that the implied risk-neutral probabilities distribution is not dependent on the prior guess distribution. Ait-Sahalia and Lo (1998) also estimate an option pricing formula from S&P 500 option prices nonparametrically by using the kernel regression method. The option pricing function is obtained numerically also according to Breeden and Litzenberger (1978)'s result. Option prices are calculated as a weighted average of the observed option prices with the underlying variables lying in a neighborhood of the one to be calculated. A suitable kernel function is chosen as the weighting function (typically a probability density function in that probability density functions integrate to one).

In summary, parametric methods need to assume relations between variables or to assume statistical parameters such as skewness, kurtosis, and volatility. This inevitably makes parametric methods inferior due to the lack of sufficient flexibility. Nonparametric methods are much more flexible comparatively.

3 Wavelets: a brief overview

In this paper we propose an alternative to the methods we reviewed above: i) we estimate the implied risk-neutral MGF instead of the risk-neutral PDF; ii) we utilize wavelets in our approach to represent and estimate the implied

MGF function.

Although wavelets have not been extensively applied in the financial and economic field, there is a growing literature in this regard. Ramsey (1999) provides for an extensive review on using wavelet analysis to financial and economic data. We give some specific examples of applications below.

There are mainly three types of applications using wavelets in finance and economics.

1. The first kind of application of wavelet analysis is multi-resolution analysis or time scale analysis (or time-scale decomposition), which is powerful in revealing the potential relationship between the economic variables and in improving forecasts. An early key article in this regard was that by Davidson, Labys, and Lesourd (1998), where the authors apply multi-resolution analysis on US commodity price behavior and obtain information on both the time location and the time scale of price movements. In this paper, the authors also mention that wavelet analysis may help to forecast price movements. This point was proven in Murtagh, Starck, and Renaud (2004) where the authors examine several wavelet applications in time series prediction. After studying wavelet-based multiresolution autoregression models and single resolution approaches as well, the authors find that wavelet-based multiresolution approaches outperform the traditional single resolution approach in forecasting. Ramsey and Lampart (1998a) also use wavelets to analyze the relationship between the expenditure and income at six different time scales and find that the relationship varies across time scales. Further, the authors confirm that (pg.23) "the time-scale decomposition is very important for analyzing economic relation-

ships and that a number of anomalies previously noted in the literature are explained by these means". See Ramsey and Lampart (1998b) for a similar example in analyzing the relationship between money and domestic product. In subsequent work, Connor and Rossiter (2005) provide a wavelet-based scale analysis approach to analyze the commodity prices motivated by the fact that "the dynamics of commodity markets have always been influenced by the interactions of traders with different time horizons, who react to the arrival of new information in a heterogeneous manner." Mitra (2006) also exploits wavelets to do multi-resolution analysis on the econometric relationship between money, output and price in the Indian macro economy. The author claims that interesting aspects of the relationship among the three fundamental macroeconomic variables are revealed. More examples can be found in Gençay, Selçuk, and Whitcher (2002), Capobianco (2002), Yousefi, Weinreich, and Reinarz (2005).

2. The second type of application is to de-noise the time series data so that market trends or baselines can be observed easily and clearly. This is actually a subsection of the first type of application. For example, Gao and Ren (2005) use wavelets to analyze the highly erratic Shanghai Stock Market Index and find it effective in suppressing the noise in the market index. Therefore, the market baseline trend is demonstrated successfully. In the same year, Antoniou and Vorlow (2005) also apply wavelets to de-noise the FTSE100 stock returns time series and find evidence of "non-periodic cyclical dynamics". More examples can be found in Gençay, Selçuk, and Whitcher (2002).

3. The third application lies in function approximation. For instance, in Park, Vannucci, and Hart (2005), a wavelet-based Bayesian method is

exploited in function estimation. The authors find that "the wavelet procedure appears to do a very good job at estimating both the function and the other parameters of the model, for all directions and noise levels considered in the study". Furthermore, the comparison with other existing methods suggests that the wavelet-based Baysian method outperforms the splines-based Bayesian approach of Antoniadis, Gregoire, and McKeague (2004).

Besides these applications, wavelets are used to design tracking portfolios for equity funds and pricing exotic equity derivatives in Zapart (2003). Furthermore, the author compares the wavelet method with the standard linear correlation techniques and finds that the wavelet method offers better performance in designing tracking portfolios.

While wavelets have many useful properties, in this paper we are only interested in one of the most basic features of the wavelet, i.e. to represent or approximate other functions. Different wavelets have different strengths and weaknesses in approximating different functions according to the different characteristics of the wavelets and the functions to be approximated. In our research, we tried several wavelets, including the Haar wavelet (Fig.1), the Franklin wavelet (Fig.2), and the Shannon wavelet (Fig.3). Finally, we find that the Franklin wavelet requires the smallest number of terms to approximate the function at the same level of goodness of fit among all the wavelet functions we consider. Therefore, we use the Franklin wavelet to derive the risk-neutral MGF. Our objective in this paper is to use wavelets to approximate the implied risk-neutral MGF from option prices. With the estimated MGF, we will further execute out-of-sample tests to demonstrate how well the wavelet method performs in approximating functions with unknown functional forms.

4 Theoretical primitives

4.1 MGF

The MGF of a continuous random variable x is defined as:

$$M(s) = \int_{-\infty}^{\infty} p(x)e^{-xs}dx, \tag{1}$$

where $p(x)$ is the PDF of x and s is complex value in the complex plane. For a discrete random variable, its MGF is defined as

$$M(s) = \sum_{x=-\infty}^{\infty} p(x)e^{-xs}. \tag{2}$$

Inversely, the PDF is uniquely determined by the inverse Laplace transform of the MGF. In the risk-neutral world, the same relationship also holds.(see appendix for definitions for Laplace transform and inverse Laplace transform)

4.2 The wavelet method

As the name literally suggests, a wavelet is a function which looks like a small wave. It is localized over a short interval. In other words, the function values are all zero except on that short interval. The graph of the wavelet oscillates around its average value (zero) over a short distance, or the oscillations may damp out very fast outside the short distance. Generally speaking, wavelets must satisfy three criteria: firstly, a wavelet must be square integrable; secondly, the Fourier transform $\hat{\psi}(f)$ of the wavelet function $\psi(t)$ should satisfy the condition (Addison, 2002, pg. 9): $\int_0^\infty \frac{\left|\hat{\psi}(f)\right|^2}{f} df < \infty$; and third, the integral of the wavelet must be zero, which ensures the oscillatory shape of the wavelets.

Unlike Fourier series which have only sine and cosine basis functions, there are different wavelet basis functions. Let us consider the simple case of a so called Haar wavelet. The Haar mother wavelet is defined as follows:

$$\psi(t) = \begin{cases} 1 & \text{if } 0 \leq t < \frac{1}{2} \\ -1 & \text{if } \frac{1}{2} \leq t < 1 \\ 0 & \text{otherwise} \end{cases} . \tag{3}$$

The function looks like a square wave. It has non-zero values over the short interval [-1,1] and it disappears outside of this range. Wavelets are well known for their remarkable abilities of approximating functions. Any function belongs to $L^2(\mathbb{R})$ can be represented as a linear combination of wavelet functions generated from the so called mother wavelet.

Basically, two types of manipulations can be performed on the mother wavelet to change its shape and position and to have it generate other wavelets. The first type of manipulation is called dilation (scaling), which means that the wavelets may be squeezed or stretched. Another type of the manipulation is translation, by which we shift the wavelets horizontally. See Fig.1 for the example with Haar wavelet and its dilated and translated versions. The one on the top in Fig.1 is the mother Haar wavelet. The middle ones show the squeezed and stretched wavelets to half and double of their original width of the mother wavelet respectively. And the bottom ones in that figure show the right and left shifted wavelets. These wavelets are called generations of the mother wavelet $\psi(t)$. To generalize this, for any arbitrary wavelet function $\psi(\cdot) \in L^2(\mathbb{R})$, their generations $\psi_{l,k}(\cdot)$ are given by: $\psi_{l,k}(t) \equiv 2^{\frac{l}{2}}\psi(2^l t - k),\ l, k = 0, \pm 1, \pm 2, ...$ The parameter l determines the size of dilation or contraction of the wavelet and the parameter k governs the movement of the wavelet along the horizontal axis.

The wavelet functions $\psi_{l,k}(t)$ are orthogonal to each other and are nor-

malized. Therefore, $\psi_{l,k}(t)$ form an orthonormal wavelet basis for $L^2(\mathbb{R})$. Having defined the wavelet basis, we can now represent any square integrable function $x(t)$ by adding up wavelet basis functions $\psi_{l,k}(t)$ over all integers l and k:

$$x(t) = \sum_{l=-\infty}^{\infty} \sum_{k=-\infty}^{\infty} T_{l,k}\psi_{l,k}(t); \tag{4}$$

where $T_{l,k}$ are the wavelet coefficients and can be obtained through convolution of the function $x(t)$ and the basis functions $\psi_{l,k}(t)$:

$$T_{l,k} = \int_{-\infty}^{\infty} x(t)\psi_{l,k}(t)dt. \tag{5}$$

It may seem to be quite challenging to estimate the unknown function $x(t)$ using wavelet functions since we need to add up an infinite number of functions together to get the function represented without information loss. Fortunately, the coefficients $T_{l,k}$ converge to zero quickly enough when the parameters l and k increase to infinity so that we can just ignore those coefficients. Moreover, in our context, we do not need to back out the risk-neutral MGF as it fully coincides with the true risk-neutral MGF. What we need is just an approximation which does not deviate from the true function too much so that it can be used to price other contingent claims and provide the information we need.

As we said before, the Franklin wavelet function will be applied in our paper. Although Franklin mother wavelets are very complicated to deal with, they can be induced from a simple hat function defined by $h(t) = (1 - |t|)1_{[-1,1]}(t)$, with its Laplace transform given by $m_h(s) = (\frac{e^{s/2} - e^{-s/2}}{s})^2$. The dilated and translated versions of the hat function are given by $h_{l,k}(t) \equiv 2^{\frac{l}{2}} h(2^l t - k),\ l, k = 0, \pm 1, \pm 2, ...$ In consequence, we may approximate function $x(t)$ in terms of $h_{l,k}(t)$ instead of $\psi_{l,k}(t)$ following the Eq.4.

For a more detailed review on wavelets, see Hubbard (1998)for a very interesting introduction. Chui (1992) is an excellent book on the basics of wavelets. More formal and thorough presentations and explanations on wavelet theory can be found in Daubechies (1992) and Bachman, Narici, and Beckenstein (2002).

5 The model and methodology

5.1 The model

Our research in this paper is based on the work by Ma (2006b). The author derives a closed form formula for European call options in a particular parameterization of the economy, which is a generalization of many option pricing models in the existing literature. Based on the assumption that the moment generating function for $\ln S_T$ (the logarithm of the time T underlying asset price) is well defined, the formula has the following expression:

$$C_t(S_t, X, T) = Xe^{-r(T-t)}\mathcal{L}^{-1}\{\Phi_{T-t}(s)\}(\ln\frac{X}{S_t}); \tag{6}$$

where t is the current time; the operation symbol $\mathcal{L}^{-1}$ denotes the bilateral inverse Laplace transform operator (see appendix for more details); C_t is the time-t equilibrium price of the European call option; S_t is the underlying asset price at time t; X is strike price; T is the maturity date; r is the continuously compounded risk free interest rate; and $\Phi_{T-t}(s) \equiv \frac{\Theta^{T-t}(s)}{s(s+1)}$, where s is a complex value with $Re(s) \in (x^*, -1)$, and $\Theta^{T-t}(s)$ is the risk-neutral moment generating function of the logarithmic return $\ln\frac{S_T}{S_t}$. When $T - t = 1$, $\Theta(s)$ is the risk-neutral MGF for the rate of return per unit of time.

This model can be derived as follows (Ma, 2006b). Let $y = \ln S_T$; $G(e^y) = (e^y - X)^+$ denotes the payoff of the option; $p(y)$ denotes the risk-neutral probability density function for y; we have the following:

$$\begin{aligned}
& e^{r(T-t)}C_t(S_t, X, T) \\
= & \int_{\mathcal{R}} p(y)G(e^y)dy \\
= & \int_{\mathcal{R}} \mathcal{L}^{-1}\{S_t^{-s}\Theta^{T-t}(s)\}(y)G(e^y)dy \\
= & \int_{\ln X}^{\infty}(e^y - X)[\frac{1}{2\pi i}\int_{\sigma-i\infty}^{\sigma+i\infty}\Theta^{T-t}(s)e^{(y-\ln S_t)s}ds]dy \\
= & \frac{1}{2\pi i}\int_{\sigma-i\infty}^{\sigma+i\infty}S_t^{-s}\Theta^{T-t}(s)[\int_{\ln X}^{\infty}e^{sy}(e^y - X)dy]ds \\
= & \frac{1}{2\pi i}\int_{\sigma-i\infty}^{\sigma+i\infty}S_t^{-s}\Theta^{T-t}(s)[\frac{X^{s+1}}{s(s+1)}]ds \\
= & \frac{X}{2\pi i}\int_{\sigma-i\infty}^{\sigma+i\infty}\Phi^{T-t}(s)(\frac{X}{S_t})^s ds \\
= & X\mathcal{L}^{-1}\{\Phi^{T-t}(s)\}(\ln\frac{X}{S_t}), \sigma \in (x^*, -1) \qquad (7)
\end{aligned}$$

The second equality follows from the fact that the moment generating function for $y = \ln S_T$ is given by $S_t^{-s}\Theta^{T-t}(s)$, where $\Theta^{T-t}(s)$ denotes the moment generating function for $\ln\frac{S_T}{S_t}$. The sixth equality follows by denoting $\Phi^{T-t}(s) \equiv \frac{\Theta^{T-t}(s)}{s(s+1)}$.

As a special case, the 1973 Black-Scholes formula with a constant dividend-equity ratio l can be obtained by substituting the risk-neutral MGF

$$\Theta(s) = e^{-(r-l-\frac{\sigma^2}{2})s+\frac{\sigma^2}{2}s^2} \qquad (8)$$

for the rate of annual return into formula 6, where r represents the drift, and σ stands for the volatility for the random underlying stock prices.

5.2 Methodology

In this section, we explain how we perform the Monte Carlo simulation experiments to examine the performance of the wavelet estimation method for the risk-neutral moment generating function. The simulated option prices are calculated based on the benchmark Black-Scholes formula. Then we pretend that we are not aware of the fact that the option prices are obtained from the Black-Scholes formula, and we estimate the risk-neutral MGF from the option prices using the wavelet method based on Ma (2006b)'s option pricing model. The estimated risk-neutral MGF is finally plugged into the general option pricing function so that we may compare it with the Black-Scholes formula to examine the accuracy of the wavelet method. Note that our model does not assume that the Black-Scholes model actually holds in the real market. The Black-Scholes model is just employed as a benchmark in our paper to demonstrate the effectiveness of our wavelet method. Therefore, even if the options in the market were actually determined by some other option pricing models which might even be unknown to us, we can still back it out using wavelets as well since we place no prior restrictions on the stochastic price process or on the risk-neutral MGF of the underlying asset .

The experiments are conducted as follows:

1. For a given underlying asset with price S_t at time t, generate N options based on the Black-Scholes model. The N options have different strike prices $X = \{X_1, X_2, ..., X_N\}$, with a same time-to-maturity T. Calculate the corresponding option prices $C^{bs} = \{C_1^{bs}, C_2^{bs}, ..., C_N^{bs}\}$ using the Black-Scholes formula, assuming the risk-free interest rate r and the volatility of the underlying asset σ are constant and already

known.

2. Given a set of scale and shift parameters, estimate the risk-neutral moment generating function $\hat{\Theta}(s)$ of the yearly logarithmic return of the underlying asset from the data set $\{S_t,\ X,\ T,\ C^{bs}\}$ using wavelet analysis. Then we calculate the fitted option prices using Eq.6 with the derived $\hat{\Theta}(s)$. Let $C^w = \{C_1^w, C_2^w, ..., C_N^w\}$ denote the fitted wavelet-based option prices. Compare C^w with C^{bs} to get the in-sample goodness of fit.

3. Test the out-of-sample forecast ability: select another data set $\{S_t',\ X',\ T', C^{bs'}\}$. Calculate the wavelet based option prices $C^{w\prime}$ with the derived risk-neutral moment generating function $\hat{\Theta}(s)$. Compare $C^{w\prime}$ with $C^{bs'}$ to find out the out-of-sample forecast deviation.

Among the three steps above, Step 2 is the key one. We discuss this step in detail below. The algorithm used to find the coefficients of a set of wavelets that fit the data C_w to C_{bs}, is suggested by Ma (unpublished manuscript, page 245-246). The following explains how we may use wavelets to represent the risk-neutral MGF.

For any arbitrary mother wavelet function $\psi(\cdot) \in L^2(\mathbb{R})$, its generation

$$\psi_{l,k}(x) \equiv 2^{\frac{l}{2}}\psi(2^l x - k),\ l, k = 0, \pm 1, \pm 2, ... \tag{9}$$

form an orthonormal basis for $L^2(\mathbb{R})$. Let $m_\psi(s)$ and $m_{l,k}(s)$ denote the Laplace transform of $\psi(x)$ and $\psi_{l,k}(x)$ respectively, where $l, k = 0, \pm 1, \pm 2, ...$ Then we have: $m_{l,k}(s) = 2^{-\frac{l}{2}} e^{-\frac{ks}{2^l}} m_\psi(\frac{s}{2^l}), l, k = 0, \pm 1, \pm 2, ...$

Assuming that the probability density function $p(x)$ of a random variable x belongs to $L^2(\mathbb{R})$, we may expand $p(x)$ in terms of the orthonormal wavelet basis:

$$p(x) = \sum_l \sum_k a_{lk} \psi_{l,k}(x); \tag{10}$$

where $x = log(\frac{S_T}{S})$.

Perform Laplace transformation on both sides of Eq.10, we get $\Theta(s) = \sum_l \sum_k a_{lk} m_{l,k}(s), Re(s) \in (x^*, 0]$; where $\Theta(s)$ is the risk-neutral MGF of random variable x, and it is equal to the Laplace transform of the risk-neutral PDF $p(x)$.

To estimate the risk-neutral MGF with a known historic or simulated data set $\{S, X_i, T, C_i\}, i = 1, 2, ...N$, where N is the length of the data vector, S is the underlying security price, C_i is the corresponding option price calculated on the specified underlying asset price S, strike price X_i, time to maturity T, we may follow the procedures described below:

1. For positive integers L and K, truncate the coefficients by setting $a_{lk} = 0$ for all $|l| > L$,and $|k| > K$. Set $\theta_{L,K} \equiv \{a_{lk}\}_{l \leq L, |k| \leq K.}$

2. Given the collection of simulated data set,$\{S_i, X_i, T_i, C_i\}$, we estimate the unknown coefficients $\theta_{L,K}$ by taking the minimum of the sum of the squared error between the true option prices C_i^{bs} and the estimated prices C_i^w,which is obtained by substituting $\hat{\Theta}(s|\theta_{L,K})$ into formula 6.

3. Go to step 1 with $L \rightarrow L+1$ and $K \rightarrow K+1$ until $\sum_i (C_i^{bs} - C_i^w)^2 < \varepsilon$, for any arbitrary $\varepsilon > 0$.

During the process of the experiments, we find there are several problems with the above algorithm. First, with the increasing of the scale and shift parameters L and K, the time for the process of searching iteration increases dramatically, because the number of function evaluations increases geometrically. Second, the increasing of the parameters require more equa-

tions (more observed data) to do the optimization, but during the process, it always runs out of data before it can reach the optimization. Therefore, we let the scale parameter L fixed at some value, for example let $L = l = 3$, and let shift parameters k change from $-K$ to K. We change the above step 3 into two steps as follows:

- Go to step 1 with $K \rightarrow K + 1$ until $\sum_i (C_i^{bs} - C_i^w)^2 < \varepsilon$, for any arbitrary $\varepsilon > 0$.
- If the fitting result improves very little with the increase of $K \rightarrow K+1$ so that the optimization process does not terminate within a reasonable time duration, increase $L \rightarrow L + 1$, and repeat the above steps until a satisfactory fitting result is obtained. This optimization process yields an estimation of the risk-neutral MGF:

$$\hat{\Theta}(s) = \sum_{|l|=L} \sum_{|k| \leq K} \hat{a}_{lk} m_{lk}(s); \tag{11}$$

After solving the above problem about process speed, we still face another problem: how to effectively search suitable scale and shift parameters l, k for the wavelet series which compose the risk neutral moment generating function quickly and effectively. First, let's assume that we have chosen a suitable scale parameter l. According to the relationship between the PDF and the MGF, the estimated coefficients $\hat{a}_{lk}$ and corresponding wavelet function can also be used to form the risk-neutral PDF of the yearly logarithmic return of the underlying asset. Therefore, we may be able to select the appropriate initial scale and shift parameters according to the interval of yearly logarithmic returns $x = ln(\frac{S_1}{S_0})$, which lies typically in the interval $[-0.7, 0.7]$. Any wavelet has a short extension, for example, with the Franklin wavelet, its hat function has a closed and bounded interval between

$[-1, 1]$, and it disappears outside this interval. Therefore, according to Eq.9, for $\psi_{l,k}(x)$ to be effective in composing the probability density function, we need to calibrate the scale and shift parameters so that $-1 \leq 2^l x - k \leq 1$. Therefore, for a given scale parameter l, the shift parameters k should lie in the interval $[2^l x_{\min} - 1, 2^l x_{\max} + 1]$. Typically we may assume $x_{\min} = -0.7$, $x_{\max} = 0.7$, therefore

$$k \in [-0.7 * 2^l - 1, 0.7 * 2^l + 1]. \tag{12}$$

One point should be noted that the scale parameter determines the resolution of the estimated risk-neutral MGF. The larger the scale parameter, the finer the estimated risk-neutral MGF provided that the shift parameters are adequate enough. And according to 12, we need relatively more shift parameters k to apply the approximation. And this will also cost more time for the execution process. On the contrary, we may also get a feasible solution for the least squares estimation within several minutes with small scales l. However, this is obtained at the cost of fitting accuracy.

6 Simulations and experimental results

We perform constrained least squares estimation in this section. There are several restrictions for the call pricing function:

$$C(S_t, X, \tau, r_t) = e^{-r_{t,\tau}\tau} \int_X^\infty (S_T - X) p(S_T | S_t, \tau, r_t) dS_T. \tag{13}$$

First, the probability density must be non-negative. Second, the integral of the probabilities over the possible terminal asset price should be equal to one. Third, the call option pricing function should be monotonically decreasing with respect to the strike price, which means that the first derivative of the pricing function with respect to strike prices should be negative. And

fourth, the call pricing function should be convex with respect to strike prices, indicating that the second derivative of the pricing function with respect to strike prices should be positive.

Obviously, the optimization process with four restrictions requires quite a lot of computing time. Fortunately, the latter two restrictions can be inferred from the first two. The following demonstrate how the latter two constraints can be achieved from the previous two. By differentiating the above call price function with respect to the strike price, we get

$$\frac{\partial C}{\partial X} = -e^{-r_t\tau} \int_X^\infty p(S_T|S_t,\tau,r_t)dS_T; \tag{14}$$

since

$$p(S_T|S_t,\tau,r_t) \geq 0, \tag{15}$$

and

$$\int_0^\infty p(S_T|S_t,\tau,r_t)dS_T = 1, \tag{16}$$

therefore $0 \leq \int_X^\infty p(S_T|S_t,\tau,r_t)dS_T \leq 1$, and we get the third constraint:

$$-e^{-r_t\tau} \leq \frac{\partial C}{\partial X} \leq 0. \tag{17}$$

To get the fourth constraint, twice differentiate the call price function:

$$\frac{\partial^2 C}{\partial X^2} = e^{-r_t\tau} p(X|S_t,\tau,r_t) \geq 0. \tag{18}$$

This is non-negative since both $e^{-r_t\tau}$ and $p(S_T|S_t,\tau,r_t)$ are non-negative.

From the above, we can see that the first two constraints 15 and 16 about the probability density function are enough to ensure the monotonicity 17 and convexity 18 of the call price function. Therefore, we can only impose the first two constraints on the wavelet estimator.

We perform three experiments in this section by generating historic option prices with time-to-maturity of one year, one month and six months respectively.

6.1 Time-to-maturity: one year

Let $\{X_1,X_{2,...,}X_n\}$ denote a strike price sample with size n. We assume that we observe nine call options with underlying stock price $S = 100$, and the strike prices are equally spaced between 80 and 120. Other variables are specified as follows: time to maturity $T = 1$, risk-free interest rate $r = 0.05$, volatility $\sigma = 0.2$. For simplicity, we assume further for the moment that there are no dividends paying on the underlying stock. Let C^{bs} and C^{w}denote respectively the true option prices based on the Black-Scholes model and the wavelet estimated option prices based on Ma's model. Given the information above, we perform wavelet analysis to estimate the risk-neutral MGF. We find that we are able to estimate the true call pricing function with only nine Franklin wavelet hat functions with scale parameter $l = 3$ and shift parameters varying from $k = -4 : 4$.

The estimation errors are reported in the first row in Panel A of Table 1, from which we can see that the sum of squared errors between C^{bs} and C^{w} is $1.4441 * 10^{-4}$ and the maximum of the squared errors is $3.8171 * 10^{-5}$. And in fact, all the numbers in the first two rows of Panel A of Table 1 are all very small and almost close to zero. Fig.4 shows the overall image of the true option pricing function and the estimated function. Indeed, a plot of the difference between the true option prices and the estimated prices are so small that it cannot be distinguished easily by eye. The estimated prices seem to coincide with the Black-Scholes prices. Both Table 1 and Fig.4

demonstrate that the estimated call pricing function produces nearly the same call prices as the Black-Scholes function does. The approximated coefficients are $\{\hat{a}_{lk}\}$=[0.0482 0.2034 0.0554 0.5405 0.7500 0.6005 0.4971 0.0220 0.1112] ordered for the Franklin wavelet hat function with scale parameter $l = 3$ and shift parameters $k = -4 : 4$.

The Black-Scholes MGF and the approximated MGF for the annual logarithmic return $\ln(\frac{S_1}{S_0})$ (S_0 is the current spot underlying asset price and S_1 is the stock price in one year) are plotted in Fig.5. This figure is produced by calculating the value of the function $\Theta(s)$ and $\hat{\Theta}(s)$ for complex values s varying from $-2 - 20i$ to $-2 + 20i$ with imaginary unit i as the increment. We plot the two risk-neutral MGF's with the real part of the complex value s on the X-axis and the imaginary part on the Y-axis. Fig.5 shows that the shape of the estimated risk-neutral MGF is close to the true one.

The Black-Scholes model assumes that the stock prices follow a log-normal distribution. Therefore, we have the following distribution for the annual logarithmic return $x = \ln(\frac{S_1}{S_0})$:$P(x) = \frac{1}{\sigma\sqrt{2\pi}} e^{-(x-(\mu-\frac{\sigma^2}{2}))^2/2\sigma^2}$. We have the normal distribution with $\mu = 0.05$, and $\sigma = 0.2$ shown in solid curve in Fig.6. The estimated risk-neutral probability density function for $\ln(\frac{S_1}{S_0})$ can be obtained by using the estimated coefficients $\{\hat{a}_{lk}\}$: $\hat{p}(x) = \sum_l \sum_k \hat{a}_{lk}\psi_{l,k}(x)$; which is plotted in stars in Fig.6. The integral of the estimated risk-neutral PDF through the constrained optimization over the X-axis is equal to one.

The first derivative of the approximated call pricing function with respect to the strike price are all negative and lie within the area $(-0.9, -0.2)$, since $-e^{-r_t\tau} = -0.9456$ for $r = 0.05$ and $\tau = 1$, the area that the first derivative falls in keeps in line with the constraint 17 above. Moreover, the second

derivative of the approximated call pricing function with respect to the strike price are all positive, indicating that the call pricing function is convex.

Having obtained the estimated risk-neutral MGF, we are interested in pricing out-of-sample options. This is done as follows. The out-of-sample options are divided into three groups. The first group has time-to-maturity different from in-sample options while the underlying asset price and strike prices are the same with in-sample options. The second group has both different time-to-maturity and different strike prices from those of in-sample options. The third group are those options with a different time-to-maturity, different strike prices and a different underlying stock price from those of in-sample options.

1. First, we apply the estimated risk-neutral MGF in pricing out-of-sample options with different time-to-maturity. In this case, we employ four sub-groups of out-of-sample options with time-to-maturity of one month, three months, six months and nine months respectively. We give two types of the forecasting errors between the true Black-Scholes option prices and the prices based on Ma's model using the revealed $\hat{\Theta}(s)$: the squared error $\text{err}_i^{sqr} = (C_i^{bs} - \hat{C}_i^w)^2$, and the absolute error $\text{err}_i^{abs} = |C_i^{bs} - \hat{C}_i^w|$. Panel A (excluding the first row) of Table 1 reports the out-of-sample forecasting errors including the mean, minimum, maximum, and sum of err_i^{sqr} and err_i^{abs}. The standard deviations are also be reported. We choose the group of options with time-to-maturity 84/365, which has the biggest errors, to be presented in Fig.7. From both Panel A of Table 1 and Fig.7, we may conclude that the estimated risk-neutral MGF is effective in pricing out-of-sample options with different time-to-maturity, especially those options with time-to-maturity close to the in-sample ones.

2. We test the capability of the revealed risk-neutral MGF to forecast option prices of different strike prices and different time-to-maturity as well. We change the strike prices and make them vary from 80 to 120 with one unit as the incremental size instead of 5 units as in the first case. The underlying asset prices are kept unchanged. Prices of five sub-groups out-of-sample options with five different time-to-maturity for the set of strike prices $(80 : 1 : 120)$ are calculated with both the Black-Scholes formula and Ma's formula 6. We present the pricing errors in Panel B of Table 1, from which we can see that the biggest pricing errors appear in the group with time-to-maturity of 84 days. The maximum of the squared errors is only 0.1584 among the 41 options with an option prices average of 6.8440. Following the convention in case 1, we choose this set of options to be plotted in Fig.8. From Panel B of Table 1 and Fig.8, we may draw a conclusion that the revealed risk-neutral MGF behaves well in forecasting out-of-sample options with both different time-to-maturity and different strike prices.

3. Both of the previous two cases are dealing with out-of-sample options with the same underlying asset price. In this case, we want to further the extent of out-of-sampleness, i.e., we are interested in pricing options with not only different T and different X, but also different underlying asset price S. It is of interest to see if we could price out-of-sample options with different underlying asset prices. Fortunately, we know that the risk-free interest rate r and volatility of the underlying asset prices σ can be regarded as a constant within a certain short term, for instance, within three months. Therefore, the revealed risk-neutral MGF 11which is dependent on r and σ, can also be re-

garded as unchanged within the three months. This means that we can use $\hat{\Theta}(s)$ estimated from historical data to forecast prices of options with different underlying asset prices within a certain short period. For example, the underlying asset price S_0 is now 100. We assume it will raise up to 120 two months later, and the strike prices will also change by varying from 100 to 140 with 5 units as the increment accordingly. The time-to-maturity is assumed to be one, three, six, nine months and one year respectively. Panel C in table 1 shows the out-of-sample forecast ability for the five sub-groups of options. As before, Fig.9 plots the prices of options with underlying asset price 120, strike prices X=100 : 5 : 140, and time-to-maturity $T = 84/365$. From Panel C of Table 1 and Fig.9, we see that $\hat{\Theta}(s)$ can price not only out-of-sample options with different time-to-maturity, different strike prices, but also with different underlying asset prices!

Although all of the three figures (Fig.7, 8, and 9) reflect the forecasting errors which are relatively the biggest among each main group, we can see from the figures that our estimated risk-neutral MGF $\hat{\Theta}(s)$ is doing a good job in forecasting out-of-sample options. In order to make the experiment complete, we conduct two more estimations for simulated in-sample options with time-to-maturity of one month and six months respectively.

6.2 Time-to-maturity: one and six months

Following section 6.1, we execute two more estimations by modifying the time-to-maturity of in-sample options. We set the time-to-maturity as one month and six months respectively. The other parameter settings are kept unchanged with that in section 6.1. For simplicity, we do not draw figures

for this estimation. The estimated coefficients are $\{\hat{a}_{lk}\}$ =[0.0691 0.1317 0.2498 0.4743 0.6504 0.6284 0.4106 0.1744 0.0398] when using one month options and $\{\hat{a}_{lk}\}$ = [0.0054 -0.0002 0.2557 0.5757 0.7206 0.6669 0.3938 0.1625 0.0480] when using six months options. The sum of estimation errors is 0.3096 and 0.0008 respectively. Comparing with the results in the above estimation when the in-sample options have time-to-maturity of one year, the errors are a bit larger. Furthermore, the estimated risk-neutral MGFs also deviate from the true one a bit more than the one when $T = 1$. There are probably three reasons for the estimated risk-neutral MGF from options with one month and six months maturity to deviate from the true one a bit more than the MGF estimated from options with one year maturity.

1. During the optimization process, the gradient should be calculated in each iteration. However, when the time-to-maturity is not equal to 1, the gradient is much more difficult to calculate, therefore, much larger errors will occur during the gradient calculation process. What's more, the optimization process will take longer time and also more function evaluations are needed such that the optimization will terminate because the maximum function evaluations might have been exceeded. In this case, what we will do is to restart the optimization process with the optimized coefficients obtained from the terminated optimization process as the initial restart values. We may repeat this process until we get a more satisfying result.

2. From the Eq.6, we know that to calculate the options prices, we have to do an inverse Laplace transform. Therefore, we have to integrate the $\frac{\Theta^{T-t}(s)}{s(s+1)}$ over the interval from negative infinity to positive infinity. But unfortunately, this is practically not achievable. We choose a symmetrical interval such as [-2-20i ,-2+20i], or we may increase the

interval to [-2-200i ,-2+200i], but obviously, we can not reach infinity. This may also cause some of the estimation errors.

3. For the case when in-sample options have a time-to-maturity of one month and the strike prices vary from 80 to 120, four out of nine of the options have prices less than one and near to zero. Options with prices near zero might contain relatively less information about the risk-neutral MGF than other options do, therefore using a sample containing about half of the options with prices close to zero results in a bit larger estimation errors for the risk-neutral MGF.

However, despite the relatively larger estimation errors, the estimated risk-neutral MGF still performs well in the out-of-sample forecasting. Tables 2 and 3 provide for the estimation details including both in-sample fit and out-of-sample forecast for one month and six months respectively. They report the estimation errors in the same order as that in Table 1 for the case 1, 2, and 3 for the first estimation. From the tables, we can find that the estimated risk-neutral MGF forecasts better when the out-of-sample options have time-to-maturity closer to the in-sample one. When the time-to-maturity increases, the forecast errors increase as well, although in very small steps.

7 Conclusions

In this paper, we have applied the wavelet methodology for estimating the risk-neutral MGF of the underlying asset from options prices based on the new option pricing formula developed by Ma (2006b). The most important contribution in our paper is that the wavelet method applied on Ma (2006b)'s model offers a promising alternative for pricing out-of-sample op-

tions and also for pricing other complex and illiquid derivative claims on the underlying asset, using information obtained from simulated historical data.

Our experiment mainly contains three steps. First, we simulate a data set for options by calculating the options prices using the benchmark Black-Scholes formula. Second, we pretend that we do not know the option prices are obtained from the Black-Scholes formula and we use a series of wavelet functions with different scale and shift parameters to estimate the implied risk-neutral MGF. Third, we compare the estimated risk-neutral MGF and true risk-neutral MGF to see whether the wavelet method is effective in revealing the risk-neutral MGF. We also apply the estimated risk-neutral MGF to price out-of-sample options with different times-to-maturity, different strike prices and different underlying asset prices. Through comparison between the obtained option prices from the estimated risk-neutral MGF and the true Black-Scholes risk-neutral MGF, we get strong evidence of the superior ability of the wavelet method in estimating risk-neutral MGF.

There are at least six advantages for approximating the implied MGF using the wavelet method: 1. The estimated MGF is continuous. 2. For practical purpose, it is more appealing to estimate the MGF instead of the PDF. 3. It is convenient to reveal the rich information contained in the option prices from the implied MGF. 4. Using the wavelet method allows for flexibility. 5. The wavelet method requires a relatively small sample of data. 6. The wavelet method avoids ill-posed inverse problems.

References

Addison, P. S., 2002, *The illustrated wavelet transform handbook* (Napier University).

Ait-Sahalia, Y., and A. Lo, 1998, Nonparametric estimation of state-price densities implicit in financial asset prices, *Journal of Finance* pp. 499–547.

Antoniadis, A., G. Gregoire, and I. W. McKeague, 2004, Bayesian estimation in single-index models, *Statistica Sinica* 14, 1147–1164.

Antoniou, A., and C. E. Vorlow, 2005, Price clustering and discreteness: is there chaos behind the noise?, *Physica A* 348, 389–403.

Bachman, G., L Narici, and E. Beckenstein, 2002, *Fourier and wavelet analysis* (Springer).

Bates, D., 1991, The crash of 87': Was it expected? the evidence from options markets, *Journal of Finance* 46, 1009–1044.

——— , 2000, Post-87' crash fears in the s&p 500 futures options, *Journal of Econometrics* 94, 181–238.

Black, F., and M. Scholes, 1973, The pricing of options and corporate liabilities, *Journal of Political Economy* 81, 637–659.

Bliss, R. R., and N. Panigirtzoglou, 2002, Testing the stability of implied probability density functions, *Journal of Banking and Finance* 26, 381–422.

Breeden, D. T., and R. H. Litzenberger, 1978, Prices of state-contingent claims implicit in option prices, *Journal of business* 51, 621–651.

Capobianco, E., 2002, Independent component analysis and resolution pursuit with wavelet and cosine packets, *Neurocomputing* 48, 779–806.

Chui, C. K., 1992, *An introduction to wavelets* (Academic Press).

Connor, J., and R. Rossiter, 2005, Wavelet transforms and commodity prices, *Studies in Nonlinear Dynamics and Econometrics* 9, Article 6.

Daubechies, I., 1992, *Ten lectures on wavelets* (SIAM).

Davidson, R., W. C. Labys, and J. B. Lesourd, 1998, Wavelet analysis of commodity price behavior, *Computational Economics* 11, 103–28.

Duffie, D., J. Pan, and K. Singleton, 2000, Transform analysis and asset pricing for affine jump-diffusions, *Econometrica* 68, 1343–1376.

Gao, L., and H.Y. Ren, 2005, Detect market baseline trend with wavelet analysis, *Wavelet Analysis and Active Media Technology* pp. 1497–1502.

Gençay, R., F. Selçuk, and B. Whitcher, 2002, *An Introduction to Wavelets and Other Filtering Methods in Finance and Economics* (Academic press).

Hubbard, B. B., 1998, *The world according to wavelets* (A K Peters) 2 edn.

Ma, C. H., 1992, Two essays on equilibrium asset pricing and intertemporal recursive utility, Ph.D. thesis Department of Economics,University of Toronto.

——— , 2006a, Advanced asset pricing theory, Unpublished manuscript.

——— , 2006b, Intertemporal recursive utility and an equilibrium asset pricing model in the presence of levy jumps, *Journal of Mathematical Economics* 42, 131–160.

——— , and K. R. Vetzal, 1995, Pricing options on the market portfolio with discontinuous returns under recursive utility, Mimeo University of Waterloo.

Malz, A. M., 1997, Estimating the probability distribution of the future exchange rate from options prices, *Journal of Derivatives* pp. 18–36.

Melick, W. R., and C. P. Thomas, 1994, Recovering an asset's implied pdf from option prices: an application to crude oil during the gulf crisis, *Journal of Financial and Quantitative Analysis* 32, 91–115.

Mitra, S., 2006, A wavelet filtering based analysis of macroeconomic indicators: the indian evidence, *Applied Mathematics and Computation* 175, 1055–1079.

Murtagh, F., J.L. Starck, and O. Renaud, 2004, On neuro-wavelet modeling, *Decision Support Systems* 37, 475–484.

Park, C. G., M. Vannucci, and J. D. Hart, 2005, Bayesian methods for wavelet series in single-index models, *Journal of Computational and Graphical Statistics* 14, 770–794.

Ramsey, J. B., and C. Lampart, 1998a, The decomposition of economic relationship by time scale using wavelets: expenditure and income, *Studies in Nonlinear Dynamics& Econometrics* 3, 23–42.

——— , 1998b, Decomposition of economic relationship by time scale using wavelets: money and income, *Macroeconomic Dynamics* 2, 49–71.

Rubinstein, M., 1994, Implied binomial trees, *Journal of Fiance* 49, 771–818.

Shimko, D., 1993, Bounds of probability, *Risk* 6, 33–37.

Yousefi, S., I. Weinreich, and D. Reinarz, 2005, Wavelet-based prediction of oil prices, *Chaos Solitons & Fractals* 25, 265–275.

Zapart, C., 2003, Application of the wavelet correlation measure in computational finance, in *Proceedings of the 7th joint conference on information sciences* pp. 1080–1083.

Appendix: Laplace transform

For a function $f(t)$ which is real valued and piecewise continuous on $[0, \infty)$, its Laplace transformation is a complex valued function given by

$$\mathcal{L}\{f(t)\}(s) = F(s) = \int_0^\infty f(t)e^{-st}dt; \tag{19}$$

where s is complex value in the complex plane and $\mathcal{L}$ denotes the Laplace transform operator. The inverse Laplace transform, denoted by $\mathcal{L}^{-1}\{F(s)\}(t)$, is defined as:

$$\mathcal{L}^{-1}\{F(s)\}(t) = f(t) = \frac{1}{2\pi i}\int_{c-i\infty}^{c+i\infty} F(s)e^{st}ds; \tag{20}$$

where c is a specific real number so that all singularities of $F(s)$ are to the left of it.

To introduce the Laplace transform into the option pricing model, we need not only positive t, but also negative t. Therefore, we need a so-called bilateral Laplace transform and bilateral inverse Laplace transform. The bilateral Laplace transformation of $f(t)$, denoted by $\mathcal{L}\{f(\cdot)\}(s)$, is given by

$$\mathcal{L}\{f(t)\}(s) = F(s) = \int_{-\infty}^\infty f(t)e^{-st}dt; \tag{21}$$

where $f(t)$ is defined for $t \in \mathbb{R}$, and s is a complex value in the complex plane. Let $F(s)$ denote $\mathcal{L}\{f(x)\}(s)$ and $G(s)$ denote $\mathcal{L}\{g(x)\}(s)$, we have the properties of the Laplace transform summarized as following:

1. Linearity

$$\mathcal{L}\{af(x) + bg(x)\}(s) = aF(s) + bG(s); \tag{22}$$

$$\mathcal{L}^{-1}\{aF(s) + bG(s)\}(x) = af(x) + bg(x). \tag{23}$$

2. Frequency shifting

$$\mathcal{L}\{e^{-lx}f(x)\}(s) = F(s + l), \forall l \in R; \tag{24}$$

$$\mathcal{L}^{-1}\{F(s+l)\}(x) = e^{-lt}f(x), \forall l \in R. \tag{25}$$

3. Time shifting

$$\mathcal{L}\{f(x-x_0)\}(s) = e^{-x_0 s}F(s), \forall x_0 \in R; \tag{26}$$

$$\mathcal{L}^{-1}\{e^{-x_0 s}F(s)\}(x) = f(x-x_0), \forall x_0 \in R. \tag{27}$$

4. Convolution

$$\mathcal{L}\{f(x) * g(x)\} = F(s)G(s); \tag{28}$$

$$\mathcal{L}^{-1}\{F(s)G(s)\}(x) = f(x) * g(x). \tag{29}$$

where '*' indicates the convolution operator on f and g. This operator can be defined as:

$$f * g \equiv \int_{-\infty}^{\infty} f(\tau)g(t-\tau)d\tau = \int_{-\infty}^{\infty} g(\tau)f(t-\tau)d\tau. \tag{30}$$

(Bracewell 1999, p. 25).

Table 1. In-sample and out-of-sample pricing errors for options with one-year to maturity.

In the first column of each panel, "in"denotes the in-sample test and "out"denotes the out-of-sample test. The second column shows time-to-maturity in days. The third column reports the average call option prices from the benchmark model. The summary statistics for squared and absolute errors between the simulated option prices and the prices obtained by wavelet estimator are reported in the last five columns.

	T	c_{BS}	error	mean	min	max	sum	std
				Panel A. Case 1				
in	365	12.2257	sqr	$1.6046*10^{-5}$	$2.3132*10^{-6}$	$3.8171*10^{-5}$	$1.4441*10^{-4}$	$1.2081*10^{-5}$
			abs	0.0037	0.0015	0.0062	0.0337	0.0015
out	28	6.1368	sqr	0.0341	0.0017	0.1489	0.3072	0.0518
			abs	0.1425	0.0415	0.3859	1.2829	0.1247
out	84	7.2201	sqr	0.0449	0.0048	0.1584	0.4043	0.0496
			abs	0.1859	0.0692	0.3980	1.6735	0.1079
out	168	8.8083	sqr	0.0239	0.0012	0.0879	0.2148	0.0277
			abs	0.1322	0.0346	0.2965	1.1894	0.0848
out	252	10.3156	sqr	0.0054	$4.5616*10^{-5}$	0.0250	0.0489	0.0081
			abs	0.0573	0.0068	0.1583	0.5161	0.0491
				Panel B. Case 2				
out	365	12.0025	sqr	$1.6808*10^{-5}$	$8.4748*10^{-10}$	$6.0796*10^{-5}$	$6.8912*10^{-4}$	$1.4882*10^{-5}$
			abs	0.0036	0.0000	0.0078	0.1481	0.0020
out	28	5.6946	sqr	0.0293	$3.7812*10^{-6}$	0.1489	1.2002	0.0407
			abs	0.1310	0.0019	0.3859	5.3718	0.1114
out	84	6.8440	sqr	0.0407	$2.2375*10^{-5}$	0.1584	1.6695	0.0419
			abs	0.1739	0.0047	0.3980	7.1302	0.1036
out	168	8.5008	sqr	0.0215	$2.1009*10^{-5}$	0.0879	0.8831	0.0235
			abs	0.1249	0.0046	0.2965	5.1222	0.0780
out	252	10.0524	sqr	0.0047	$4.8679*10^{-7}$	0.0250	0.1943	0.0067
			abs	0.0543	0.0007	0.1583	2.2255	0.0429
				Panel C. Case 3				
out	365	14.1573	sqr	$2.7375*10^{-5}$	$8.8791*10^{-7}$	$8.8740*10^{-5}$	$2.4638*10^{-4}$	$2.7234*10^{-5}$
			abs	0.0046	0.0009	0.0094	0.0411	0.0027
out	28	6.3313	sqr	0.0355	$1.9469*10^{-4}$	0.1500	0.3199	0.0475
			abs	0.1539	0.0140	0.3873	1.3848	0.1156
out	84	7.7913	sqr	0.0517	0.0016	0.1402	0.4655	0.0512
			abs	0.1970	0.0402	0.3744	1.7727	0.1206
out	168	9.8596	sqr	0.0272	$8.2177*10^{-6}$	0.0846	0.2450	0.0286
			abs	0.1416	0.0029	0.2908	1.2744	0.0899
out	252	11.7720	sqr	0.0057	$2.1060*10^{-5}$	0.0242	0.0509	0.0077
			abs	0.0612	0.0046	0.1556	0.5505	0.0464

Table 2. In-sample and out-of-sample pricing errors for options with 1-month to maturity

This table reports the summary statistics of the pricing errors in the same format as Table 1 for 1-year maturity.

	T	c_{BS}	error	mean	min	max	sum	std
				Panel A. Case 1				
in	28	6.1368	sqr	0.0344	0.0017	0.0860	0.3096	0.0324
			abs	0.1604	0.0408	0.2932	1.4440	0.0987
out	84	7.2201	sqr	0.0073	$1.1401*10^{-4}$	0.0257	0.0659	0.0089
			abs	0.0684	0.0107	0.1604	0.6157	0.0545
out	168	8.8083	sqr	0.0081	$7.0984*10^{-6}$	0.0238	0.0730	0.0079
			abs	0.0769	0.0027	0.1542	0.6923	0.0497
out	252	10.3156	sqr	0.0185	$6.4067*10^{-4}$	0.1071	0.1669	0.0347
			abs	0.1002	0.0253	0.3273	0.9015	0.0978
out	365	12.2257	sqr	0.0573	$7.7899*10^{-5}$	0.3103	0.5153	0.1060
			abs	0.1512	0.0088	0.5570	1.3605	0.1967
				Panel B. Case 2				
out	28	5.6946	sqr	0.0344	$5.7446*10^{-5}$	0.1016	1.4093	0.0299
			abs	0.1646	0.0076	0.3188	6.7470	0.0865
out	84	6.8440	sqr	0.0073	$3.1225*10^{-6}$	0.0261	0.3006	0.0087
			abs	0.0694	0.0018	0.1616	2.8443	0.0508
out	168	8.5008	sqr	0.0072	$3.2518*10^{-7}$	0.0238	0.2937	0.0064
			abs	0.0734	$5.7025*10^{-4}$	0.1542	3.0106	0.0426
out	252	10.0524	sqr	0.0141	$3.3319*10^{-7}$	0.1071	0.5765	0.0245
			abs	0.0892	$5.7722*10^{-4}$	0.3273	3.6576	0.0791
out	365	12.0025	sqr	0.0457	$7.3917*10^{-6}$	0.3103	1.8742	0.0819
			abs	0.1359	0.0027	0.5570	5.5710	0.1671
				Panel C. Case 3				
out	28	6.3313	sqr	0.0499	0.0011	0.1238	0.4495	0.0468
			abs	0.1909	0.0326	0.3519	1.7185	0.1232
out	84	7.7913	sqr	0.0107	$1.8593*10^{-4}$	0.0376	0.0964	0.0135
			abs	0.0847	0.0136	0.1940	0.7620	0.0631
out	168	9.8596	sqr	0.0095	$1.6785*10^{-4}$	0.0230	0.0855	0.0085
			abs	0.0849	0.0130	0.1515	0.7640	0.0508
out	252	11.7720	sqr	0.0149	$8.6825*10^{-5}$	0.0745	0.1344	0.0232
			abs	0.0976	0.0093	0.2729	0.8780	0.0780
out	365	14.1573	sqr	0.0511	$1.6016*10^{-4}$	0.2743	0.4601	0.0935
			abs	0.1471	0.0127	0.5238	1.3240	0.1821

Table 3. In-sample and out-of-sample pricing errors for options with 6-month to maturity.

This table reports the summary statistics of the pricing errors in the same format as Table 1.

	T	c_{BS}	error	mean	min	max	sum	std
				Panel A. Case 1				
in	168	8.8083	sqr	0.0001	0.0000	0.0004	0.0008	$1.3713*10^{-4}$
			abs	0.0077	0.0012	0.0207	0.0694	0.0062
out	28	6.1368	sqr	0.0212	0.0005	0.0600	0.1912	0.0214
			abs	0.1271	0.0215	0.2449	1.1435	0.0758
out	84	7.2201	sqr	0.0007	0.0000	0.0017	0.0062	$6.7554*10^{-4}$
			abs	0.0215	0.0032	0.0408	0.1931	0.0159
out	252	10.3156	sqr	0.0030	0.0000	0.0221	0.0273	0.0072
			abs	0.0335	0.0015	0.1486	0.3017	0.0464
out	365	12.2257	sqr	0.0198	0.0000	0.1089	0.1782	0.0364
			abs	0.0943	0.0033	0.3300	0.8488	0.1108
				Panel B. Case 2				
out	168	8.5008	sqr	0.0001	0.0000	0.0004	0.0034	$1.1959*10^{-4}$
			abs	0.0069	0.0000	0.0207	0.2832	0.0060
out	28	5.6946	sqr	0.0224	0.0003	0.0654	0.9185	0.0192
			abs	0.1329	0.0164	0.2558	5.4505	0.0696
out	84	6.8440	sqr	0.0007	0.0000	0.0017	0.0281	$6.4174*10^{-4}$
			abs	0.0220	0.0015	0.0418	0.9035	0.0143
out	252	10.0524	sqr	0.0001	0.0000	0.0004	0.0034	$1.1959*10^{-4}$
			abs	0.0069	0.0000	0.0207	0.2832	0.0060
out	365	12.0025	sqr	0.0155	0.0000	0.1089	0.6359	0.0272
			abs	0.0845	0.0001	0.3300	3.4658	0.0926
				Panel C. Case 3				
out	168	9.8596	sqr	0.0001	0.0000	0.0004	0.0011	$1.7544*10^{-4}$
			abs	0.0086	0.0000	0.0207	0.0770	0.0078
out	28	6.3313	sqr	0.0341	0.0002	0.0864	0.3067	0.0296
			abs	0.1581	0.0150	0.2939	1.4227	0.1011
out	84	7.7913	sqr	0.0010	0.0000	0.0024	0.0087	$9.2804*10^{-4}$
			abs	0.0266	0.0038	0.0492	0.2394	0.0169
out	252	11.7720	sqr	0.0015	0.0000	0.0099	0.0135	0.0032
			abs	0.0266	0.0035	0.0993	0.2394	0.0299
out	365	14.1573	sqr	0.0171	0.0000	0.0880	0.1536	0.0295
			abs	0.0907	0.0030	0.2967	0.8161	0.0998

Figure 1. Dilation and translation to the Haar mother wavelet

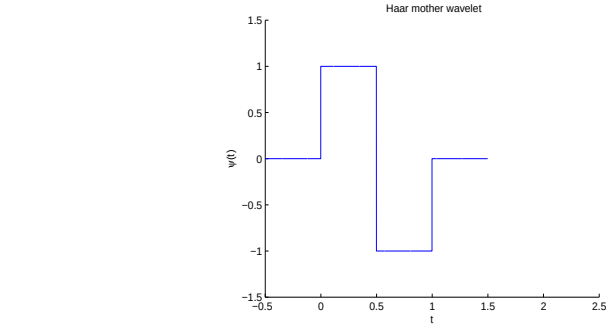

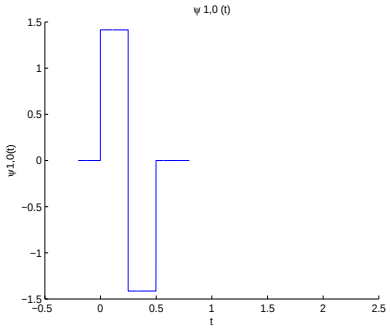

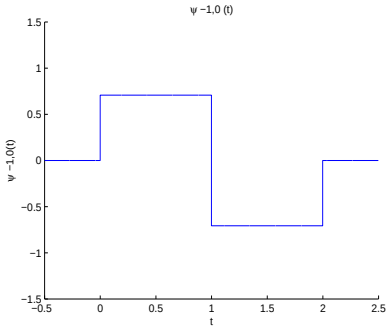

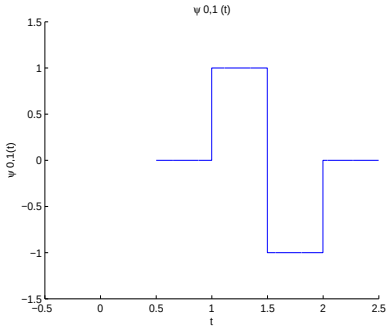

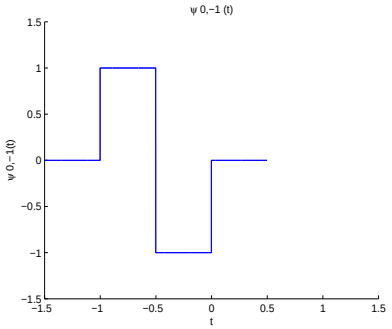

Figure 2. Franklin wavelet

Figure 3. Shannon wavelet

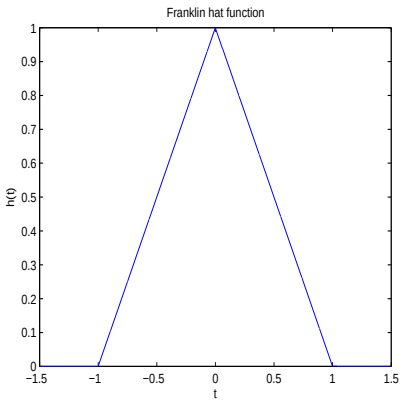

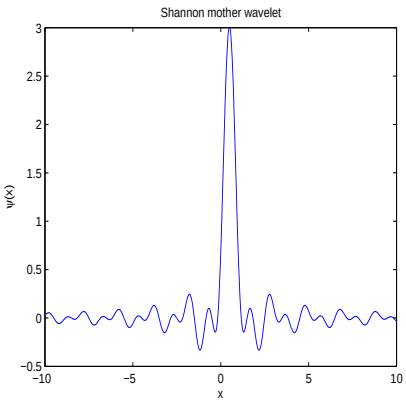

Fig 4. Simulated and fitted option prices

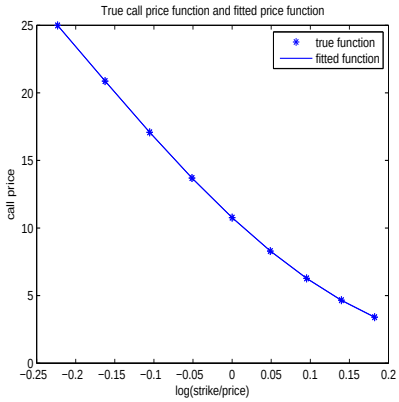

Fig 5. Simulated and fitted MGF

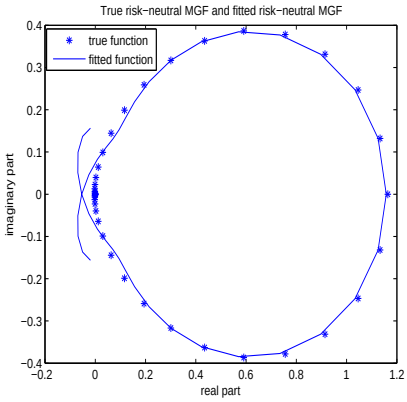

Fig 6. Simulated and fitted PDF

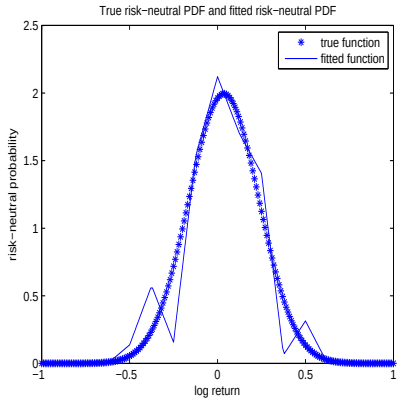

Fig 7. Out-of-sample forecast (1)

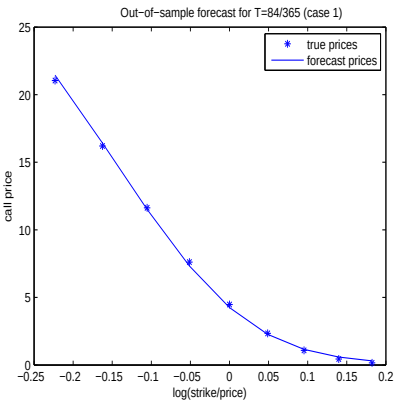

Fig 8. Out-of-sample forecast (2)

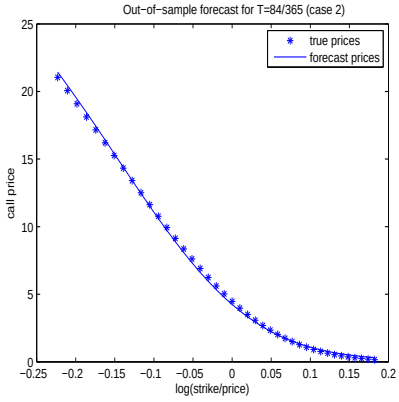

Fig 9. Out-of-sample forecast (3)